

## **Simulation and Experimental Validation of the Pressure Coefficient in Aerodynamic Profiles**

**By**

**Ing. Cristian Paúl Topa Chuquitarco, MSc**

Electromechanical Engineer, Master in Energy Efficiency, Professor of the Faculty of Engineering Sciences, Universidad Técnica Estatal de Quevedo, Los Ríos (Ecuador)

ORCID: Cristian Topa Chuquitarco, <https://orcid.org/0000-0002-2780-5488>  
[ctopac@uteq.edu.ec](mailto:ctopac@uteq.edu.ec)

**Lcdo. Leonardo Santiago Vinces Llaguno, MSc**

Degree in Physics and Mathematics, Master in Educational Management, Professor of the Faculty of Engineering Sciences, Universidad Técnica Estatal de Quevedo, Los Ríos

ORCID: Leonardo Vinces Llaguno, <https://orcid.org/0000-0002-9888-4646>  
(Ecuador) [lvinces@uteq.edu.ec](mailto:lvinces@uteq.edu.ec)

**Ing. Ángel Iván Torres Quijije, MSc.<sup>3</sup>**

Electronics and Telecommunications Engineer, Master in Connectivity and Computer Networks, Professor of the Faculty of Engineering Sciences, Universidad Técnica Estatal de

ORCID: Ángel Torres Quijije, <https://orcid.org/0000-0002-7037-7191>  
Quevedo, Los Ríos (Ecuador) [atorres@uteq.edu.ec](mailto:atorres@uteq.edu.ec)

**Ing. Byron Wladimir Oviedo Bayas, Ph.D.<sup>4</sup>**

Systems and Informatics Engineer, Master in Electrical Engineering, mention in Connectivity and Telecommunications Networks, Doctor within the official program in Information and Communication Technologies, Professor of the Faculty of Engineering Sciences, Universidad Técnica Estatal de Quevedo, Los Ríos

ORCID: Byron Oviedo Bayas, <https://orcid.org/0000-0002-5366-5917>  
(Ecuador) [boviedo@uteq.edu.ec](mailto:boviedo@uteq.edu.ec)

### **Abstract**

In order to investigate the performance of airfoils caused by boundary layer separation, this paper studies the performance using pressure coefficient simulated in ANSYS, SOLIDWORK and validated with an open cycle subsonic wind tunnel experiment. The problem is the possible lack of equipment to simulate and validate the action of aerodynamic and aeroelastic behavior due to the wind effect. In this project, the objective is focused on the pressure coefficient on a NACA 2412 airfoil of chord 16 and span 12, which was experimentally determined at Reynolds of  $0.165 \times 10^6$ , over angles of attack from  $-5^\circ$  to  $15^\circ$ . It resulted in a simulation of the pressure coefficient, where by varying the angle of attack from  $-5^\circ$  to  $15^\circ$ , the suction continuously increases at the leading edge of the top surface so that the pressure coefficient gradually decreases. It was concluded that when validating the results between ANSYS and T.V.EPN, an error of 21% was obtained, as opposed to Fluent Solidwork, which has an error of 55%.

**Keywords:** Coefficient, subsonic, card, acquisition, transducers, differential.

### **Resumen**

Con el fin de investigar el rendimiento de los perfiles aerodinámicos causados por la separación de la capa límite, este documento estudia el rendimiento mediante el coeficiente de presiones simulado en ANSYS, SOLIDWORK y validado con el experimento del túnel de

viento subsónico de ciclo abierto. El problema es la posible falta de un equipo que simule y valide la acción del comportamiento aerodinámico y aeroelástico debido al efecto del viento. En este proyecto el objetivo va enfocado al coeficiente de presión sobre un perfil NACA 2412 de cuerda 16 y span 12, que fue experimentalmente determinado a Reynolds de  $0,165 \times 10^6$ , sobre ángulos de ataque de  $-5^\circ$  a  $15^\circ$ . Resultó una simulación del coeficiente de presión, donde al variar el ángulo de ataque de  $-5^\circ$  a  $15^\circ$  la succión aumenta continuamente en el borde delantero de la superficie superior de manera que el coeficiente de presión disminuye gradualmente. Se concluyó que al validar los resultados entre ANSYS y T.V.EPN se obtuvo un error del 21% a diferencia de Fluent Solidwork que tiene un error del 55%.

**Palabras clave:** Coeficiente, subsónico, tarjeta, adquisición, transductores, diferencial.

## Introduction

The aircraft industry used to rely on computational aerodynamic agencies, such as the RAE (Royal Aircraft Establishment) of the United Kingdom and the forerunner of rational airfoil development, NACA (National Advisory Committee for Aeronautics).

NACA was a United States federal agency founded on March 3, 1915, to undertake, foster, and institutionalize aeronautical research. The agency was dissolved on October 1, 1958, to make way for the creation of NASA (National Aeronautics and Space Administration) [1].

NACA airfoils or airfoils are the cross-sectional shapes of an element that, when moving through the air, creates a pressure distribution that generates lift.

Lift is the force developed by an airfoil, moving in a fluid (air), exerted from bottom to top with a direction perpendicular to the relative wind and wingspan of the aircraft (not necessarily perpendicular to the horizon). Lift is usually represented by  $L$  (Lift = lift). The angle of incidence is the acute angle formed by the wing chord with respect to the aircraft's longitudinal axis. This angle is fixed, a design consideration that the pilot cannot change [2].

Several proposals are given for analyzing airfoils: the angle of incidence, the analysis of the angle of attack, and the generation of meshes.

When running the turbulence model, it is important to determine the appropriate size of the cells near the walls of the object of study; that is when the importance of  $Y^+$  arises, defined as a dimensionless distance. The authors worked with mesh sensitivity seeking to work with  $Y^+$  less than 1, according to Table 22, obtaining mesh sizes: coarse (0.08mm), medium (0.04 mm), fine (0.02 mm) and extra fine (0.01mm) [3].

Aviation industries use airfoil pressure simulation to ensure flight safety. Why are the simulation and experimental validation of the pressure coefficient in airfoils necessary?

To evaluate the performance of an airfoil for turbulence due to pressure, using numerical analysis models to observe the airfoil behavior with wind action.

The objective is to perform the simulation and experimental validation of the pressure coefficient of an airfoil for wind action. The articles reviewed and related to airfoil models and wind tunnels are:

Fluid-dynamic converter systems for renewable energy for Argentine Patagonia [4]; analysis of an airfoil to generate lift in the atmosphere of Mars [5][6]; design and structural

construction of a prototype of a tactical crewless aircraft with a removable modular system for the research and development center of the Ecuadorian air force in the city of Ambato, Ecuador [7]; non-stationary aerodynamics in wind turbine airfoils [8]; aerodynamic airfoils [9]; experimental evaluation of eight SZ-1500 series airfoils for low Reynolds number, experimental evaluation of eight SZ-1500 series airfoils at low Reynolds number [10]; study of some airfoils [11]; airfoil aerodynamics with multiple flow control surfaces, finite element evaluation of the airfoils [12]; finite element evaluation of drag and thrust forces on a Naca airfoil, measurement of forces in airfoil tunnels, airfoil forces in airfoil tunnel [13]; measurement of forces in a wind tunnel on airfoils manufactured by 3D printer, stationary simulations of airfoils with multiple flow control surfaces [14]; stationary simulations of rigid and flexible airfoils at ultra-low Reynolds numbers, stationary simulations of rigid and flexible airfoils at ultra-low Reynolds numbers [15]; and methodology for the modeling and simulation of fatigue tests on low power wind turbine blades [16].

The deductive method and exploratory research are used to analyze the information of the articles and adapt them to the simulation and experimental validation of the pressure coefficient in airfoils.

The result is a prototype that measures airfoil pressures by changing air speed and airflow.

Finally, the power coefficients were plotted. In addition, the pressure distributions were simulated to be compared with the data from the torque meter experiment and the six-component balance. The results showed that the pressure difference decreased substantially with increasing strength. In addition, the six-component balance and torque tester values showed smaller values than those simulated by pressure distributions.

It is concluded that in order to use the prototype, a simulated profile analysis must be performed to select the appropriate speed changes and air flows.

## **Materials and methods**

The process for the simulation and experimental validation of the pressure coefficient in airfoils is related to established formulas and parameters, which are detailed and considered for the analysis of the collected data.

### ***Materials***

In the first instance, the authors developed conceptual frameworks and information gathering strategies in which information and materials related to airfoils and their operating conditions are detailed, which were compiled through exploratory-deductive research.

### ***Wind tunnel***

The wind tunnel is an aerodynamic test facility used to study wind.

The flow patterns around the bodies and measures the aerodynamic forces between them. As shown in Fig. 1, a typical wind tunnel consists of a test section (TS) in which the model is mounted, a shrinkage cone before the test section, and a diffuser after the test section. A fan after the diffuser creates the wind [17].

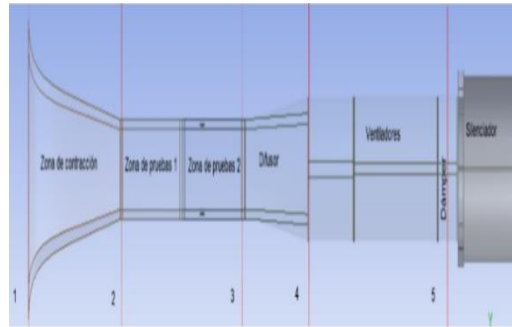


Fig. 1. Parts of the wind tunnel.

**Wind tunnel operating conditions**

These are properties such as wind speed, pressure and temperature in the shrinkage chamber and test zone. These data are shown in Table 1 [18].

**TABLE 1.** Wind tunnel operating conditions

Propiedad termodinámica	Valor	Unidad
Presión	73112	[Pa]
Densidad	1,23	[kg/m <sup>3</sup> ]
Viscosidad dinámica	1,785 E-05	[kg/m.s]
Viscosidad cinemática	1,480 E-05	[m <sup>2</sup> /s ]
Temperatura	288,15	[°K ]

**Profile evaluated in the wind tunnel**

Symmetrical profiles are recommended for low-power vertical wind turbines and are also low-cost due to their easy construction [19].

Because airfoils with high L/D ratios are sought for most applications, it is common to plot this ratio against the angle of attack or to plot the lift coefficient against the drag coefficient [20].

Naca 2412 profile of 16 cm chord and 12 cm span with 15 measuring points of 2.5 mm diameter for pressure tapping (GP), as shown in Fig. 2.

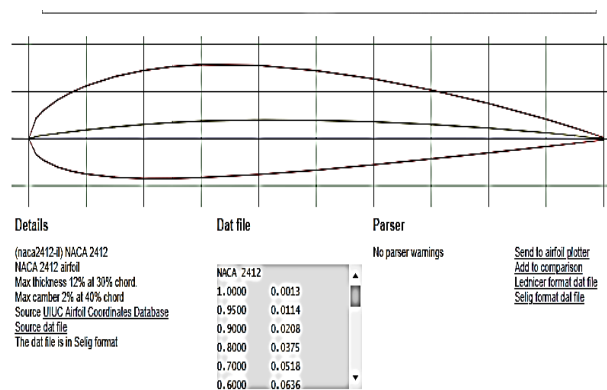


Fig. 2. Diagram of NACA 2412 profile.

## Methods

Based on the velocity data provided by the EPN wind tunnel, the airfoil simulation and analysis are performed.

### ANSYS Simulation

The simulation for comparing the parametric and experimental methods was performed in the commercial software ANSYS. The student version was analyzed since it offers the freedom to access many of the functions provided by this software. The global simulation methodology presented in Fig. 3 shows the steps followed, the information inputs and the results obtained to make an adequate comparison.

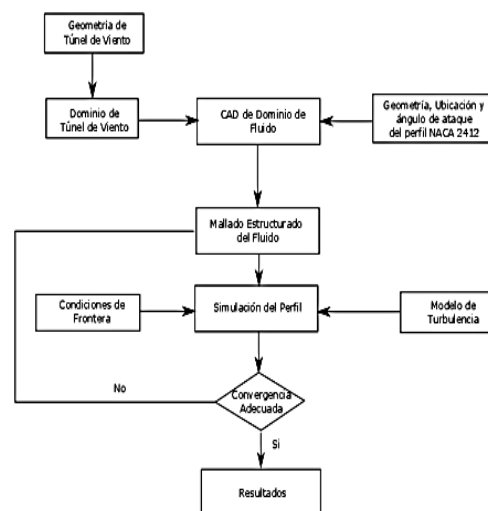


**Fig.3.** ANSYS simulation methodology

### Fluid Mastery

The geometric dimensions of the wind tunnel are measured and a 3D model of the wind tunnel is generated. Employing Boolean operations, the entire interior of the tunnel is generated as a fluid, extracted with a single body, thus having the wind tunnel domain.

The next step is the generation of a solid based on the NACA 2412 profile, which will have the specified dimensions of the actual model tested in the wind tunnel.

This will be placed inside the tunnel domain in the same arrangement as the actual model in the wind tunnel, and a Boolean extraction operation will be performed, leaving as a result, the domain fluid minus the part corresponding to the profile. This process is repeated for the angles of attack  $-5^\circ$ ,  $0^\circ$ ,  $5^\circ$ ,  $10^\circ$ , and  $15^\circ$ , which are the same as those evaluated in the wind tunnel.

All these models will be placed in independent geometry modules within ANSYS WORKBENCH.

### Structured mesh

The fluid meshing will be performed in the ICEM CFD module incorporated in ANSYS, which facilitates the generation of structured meshing with a high degree of control

of the mesh dimensions thanks to its block construction. Then, within ICEM, the next step was to import the domain fluid linked to a primary block.

From this, the study proceeded with segmenting blocks in the fluid extension of the wind tunnel and the interior. Finally, the division of the blocks is controlled to have a refinement in the vicinity of the wall with the condition of maintaining a  $Y^+$  factor less than one as visualized in Fig. 4.

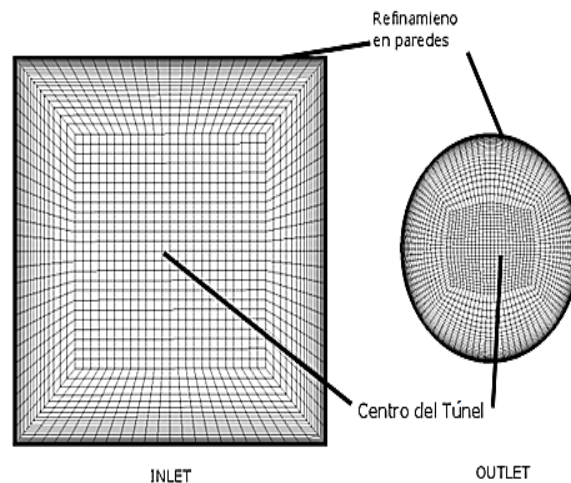


**Fig. 4.** Structured mesh at the entrance and exit of the wind tunnel.

In the generation of internal blocks, one block is made that is linked to the NACA profile contour. This will be the space that will simulate the profile wall. Meticulous care is taken with this contour because it is the most important area in the simulation, so the profile must maintain a  $Y^+$  factor of less than 1.

By generating the division of blocks in this section, a refined mesh surrounds the area of the most significant influence of the profile, which is essential to obtain good results. These parameters show a structured grid with 525600 elements, as shown in Fig. 5.

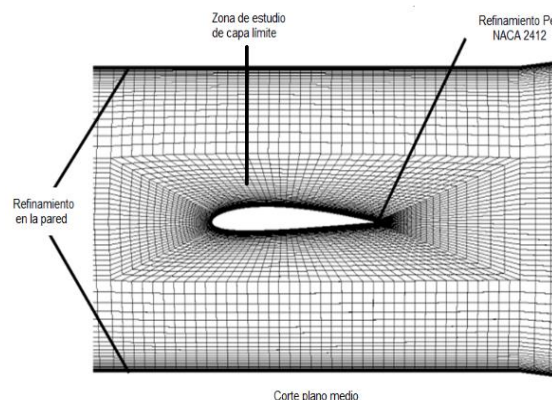


**Fig. 5.** Profile grid.

The meshing process is performed individually for the five proposed attack angles, generating the same structure for all fluid domains.

### *Simulation*

The generated grid is imported into the FLUENT module. The correct import, quality and dimensions of the mesh are checked before setting parameters. Finally, the k-ε model with improved wall treatment is selected as the viscosity model.

Since high speeds are not considered, this model will generate good results, mainly due to the proximity between the profile and the wind tunnel walls.

For working fluid, air with a density of 1.23 [kg/(m<sup>3</sup>)] and constant viscosity of 1.785e-05 [kg/(m s)] is established. Atmospheric pressure in Quito of 73112 [Pa] is a general condition.

Boundary conditions are established on all surfaces, summarized in TABLE II.

**TABLE 2.** Boundary conditions.

Área	Nombre	Condición de borde	Magnitud
Entrada	Inlet	Velocity inlet	0,9 $\left[\frac{m}{s}\right]$
Salida	Outlet	Outlet Vent	-12 [Pa], despreciando el coeficiente de perdidas
Perfil	Profile	Wall	Muro estático
Muro de túnel de viento	Wall	Wall	Muro estático

It is solved using the SIMPLEC method, with Second Order Upwind momentum conditions and First order Upwind Turbulence. The simulation has an initialization from the input. The convergence criterion is in residual values less than 1e-4 and response stability in residuals of at least 100 iterations. The simulation has 1200 iterations, but the results show convergence around 400 iterations.

### *End of process*

The results are analyzed by extracting pressures in a line of action in the center of the profile, from which the pressure coefficient was calculated and the relevant figures were created for comparison.

### *Simulation in SOLIDWORKS FLOW SIMULATION*

The CFD analysis used to compare the results obtained between the parametric and experimental methods was performed using SOLIDWORKS commercial software with the Flow Simulation analysis module. The flow diagram presented in Fig. 6 describes the methodology used in the analysis, indicating the process stages, the information inputs and the results obtained.

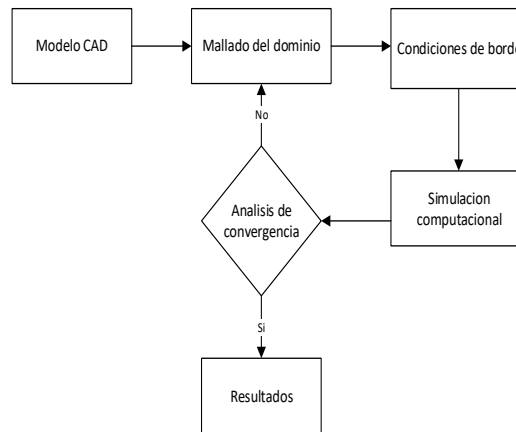


**Fig. 6.** Simulation methodology in Solid Works Flow Simulation.

**Fluid Mastery**

The fluid domain is established according to the geometric dimensions of the wind tunnel. Then, through 3D modeling, a digital version of the wind tunnel is created, an internal study analysis is applied and SolidWorks Flow Simulation automatically generates a domain with the internal geometry of the wind tunnel.

It should be noted that the NACA 2412 airfoil, which has the same dimensions as the actual model analyzed in the wind tunnel, is located in the test section of the wind tunnel. Therefore, the angles of attack used in the simulations are comprised of inclinations of  $-5^\circ$ ,  $0^\circ$ ,  $5^\circ$ ,  $10^\circ$ , and  $15^\circ$ , the same values that were evaluated in the wind tunnel.

For each inclination, a different analysis is created using different configurations for each inclination value in the angle of attack.

**Meshing**

In the Flow Simulation module of the SolidWorks design software, a meshing is performed in the calculation domain with an initial segmentation value of 0.005 m in the X and Y axes, considering a minimum of 20 cells for each channel, the tolerance criterion used is 0.000125 m, indicating a tolerance level 6 and a refinement factor on solid faces of 4 to obtain a high degree of control in the meshing dimension as shown in Fig. 7.

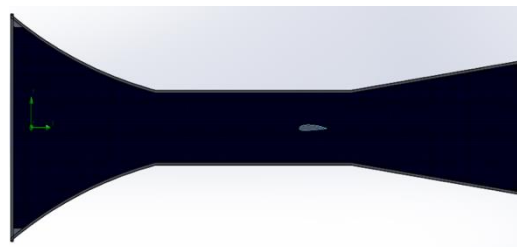


**Fig. 7.** Structured mesh at the entrance and exit of the wind tunnel.

A special mesh control must be placed on the contour of the NACA profile because this is the most important area in the data analysis, so a local mesh control is performed on the entire contour of the profile, as shown in Fig. 8.

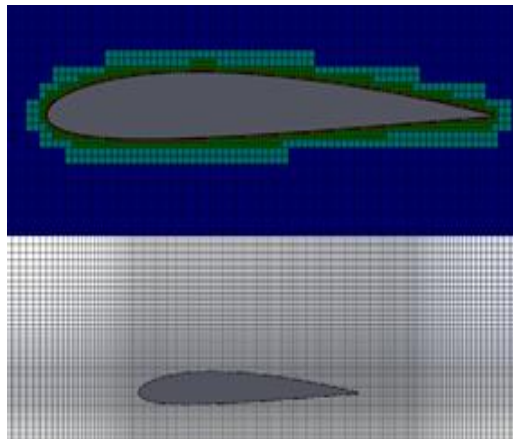


**Fig. 8.** Meshing of the profile.

Meshing for each profile at different angles of inclination is performed individually.

***Simulation***

Once the mesh is generated, the simulation begins, where the first point is to introduce the boundary conditions. These parameters can be seen summarized in TABLE 2.

The characteristics of the fluid used for the analysis indicate that it is air with a constant viscosity of  $1.785e-05$  [kg/(m s)] and a density of  $1.23$  [kg/(m<sup>3</sup>)]. Therefore, the atmospheric pressure of  $73112$  [Pa] is entered as a general condition.

The convergence analysis was run with 160 iterations of residual response. The beginning of the simulation shows 600 initial iterations and convergence of results at 300 iterations.

The initial analysis is of the stationary type, with a time variation value equal to 0. Additionally, factors such as adiabatic walls in the system and a Y-gravity of  $9.81$  [m/(sec<sup>2</sup>)] were considered.

***End of process***

The results are collected by measuring the pressure values of the points on the sketch line located at the intermediate perimeter of the profile, as shown in Fig. 9.

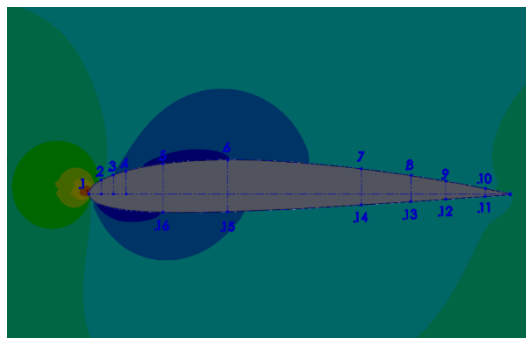


**Fig. 9.** Measurement points.

## Results

The results obtained by simulating and validating the pressure data on the NACA 2412 profile are as follows:

- The geometrical parameters of the NACA 2412 airfoil.
- Pressure distribution on the NACA 2412 profile at an angle of attack of  $-5^\circ$ .
- Pressure coefficient on NACA 2412 profile at an angle of attack of  $5^\circ$ .
- Velocity and pressure distribution NACA 2412.
- L/D vs. NACA 2412 Polar Plot.
- The angle of variation and reorientation of the NACA 2412 profile.
- Model validation using SolidWORKS.
- Modification effects on the profile due to the change of velocity.
- Modification effects on the lift curve due to pressure.

With the prototype developed, it was possible to vary the angle of attack for the airfoil, which made it possible to visualize the pressure curve and obtain the corresponding error. In the same way, thanks to the EPN wind tunnel, the inlet speed can be varied. That is why the angles and values used are the following:

The pressure distribution on the NACA 2412 airfoil at an angle of attack of  $-5^\circ$  and speed of 8m/s is shown in Fig. 10.

At  $-5^\circ$  angle of attack and a speed of 8 m/s as shown in Fig. 10, the pressure coefficient curves between Solid WORKS and TV EPN were compared and an error of 33.42% was obtained.

On the other hand, when validating between ANSYS and TV EPN, there was an error of 21.92%.

This is because the  $C_p$  values of Solid WORKS are above the TV EPN curve as opposed to the values obtained by ANSYS, which are close to the TV EPN curve.

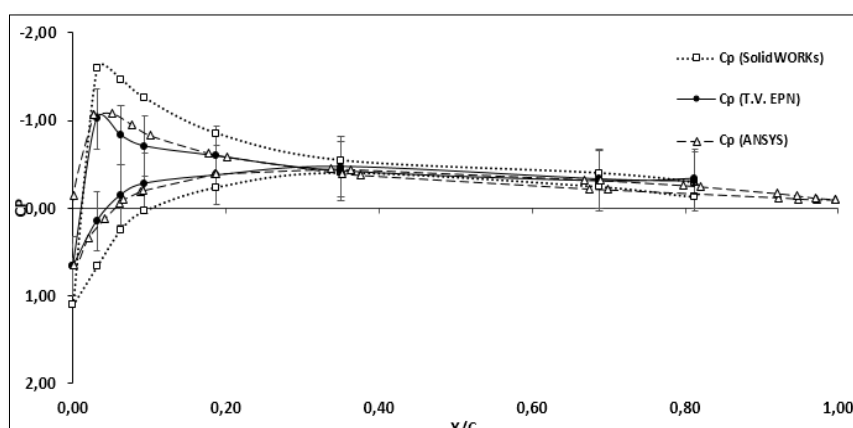


**Fig. 10.** NACA 2412 pressure coefficient, angle of attack  $-5^\circ$

When observing Fig. 11, it can be seen that varying the angle of attack from  $-5^\circ$  to  $0^\circ$  decreases the errors in the comparison between ANSYS with TV EPN to 21.05% and between Solid WORKS with TV EPN to 33.42%

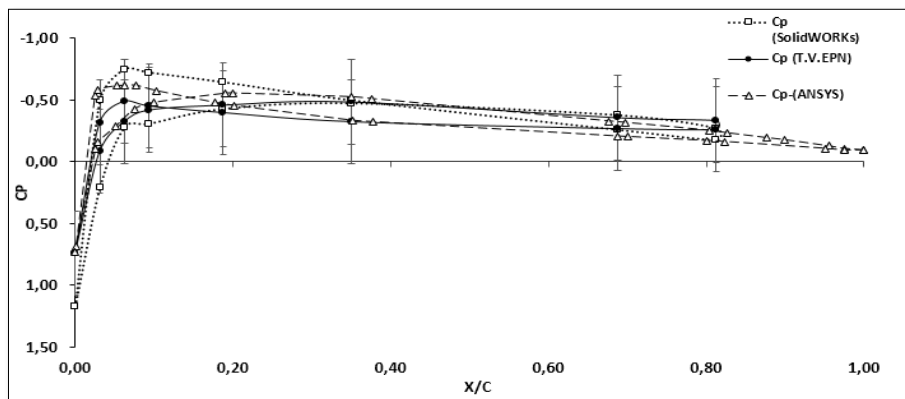


**Fig. 11.** NACA 2412 pressure coefficient, angle of attack 0°.

According to Fig. 12, as the angle of attack increases to 5°, the suction keeps increasing continuously on the leading edge of the upper surface, so the minimum pressure coefficient reached  $C_p = -0.15$  and  $C_p = -0.60$  at 0° and 5° angle of attack, respectively. However, when contrasting the numerical simulation of ANSYS with T.V.EPN, an error of 20.36 % is obtained and the error of Solid WORKS is 23.60 %.

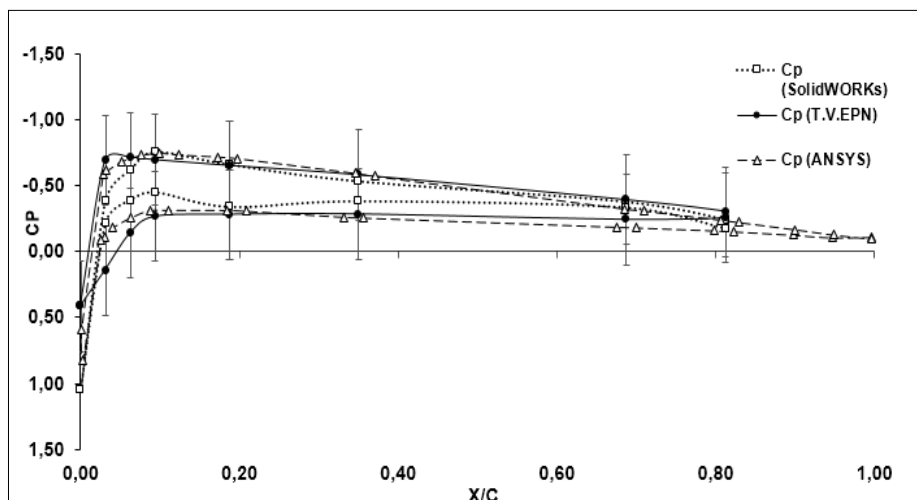


**Fig.12.** NACA 2412 pressure coefficient, angle of attack 5°.

## Discussion

This paper presented the importance of performing a simulation and experimental validation of the pressure coefficient in airfoils, which had to be implemented in a wind tunnel.

The experimental simulation considers the structural engineering, the pressure selection parameters for profiles, the TV EPN curve, and the structural mesh design at the entrance and exit of the wind tunnel in order to validate the simulated data.

The pressure values were measured in the points in the sketch line located in the intermediate perimeter of the profile in order to obtain the result values. These data allowed for calculating the pressure coefficient and these values are plotted for comparison, varying the angle of attack and speed to verify the pressure coefficient curve as needed. Thus, the most used angles are between -5° and 0°.

## **Future work and conclusions**

A future study will be planned to test the performance of different non-aerodynamic airfoils through the coefficient of pressures simulated in ANSYS, SOLIDWORKS.

- Different fin designs with different heights, pitch angles, flat shapes and airfoils have been tested and numerically optimized. The best performance improvement is achieved using a 15 cm rectangular fin with the S809 airfoil and a 45° pitch angle.
- Optimal instrumentation systems for wind tunnels were determined and selected according to the parameters velocity, free flow pressure, dimensions of the wind tunnel test section and costs. In addition, it has been found that according to the parameters and cost, it is feasible to implement the instrumentation system presented, which can be adapted for the analysis of other wind tunnels.
- Since the instrumentation systems determine the velocity, pressure, temperature and humidity variables of the air stream or the object under study, they are summarized into Static Pressure Taps, Total Pressure Rates, Hot Wire Velocity Probes and Five Hole Probes.
- However, remember that this instrumentation analyzed is applicable for open cycle subsonic wind tunnels, which operate between 0 to 30 m/s of velocity.

## **Acknowledgment**

The authors would like to thank the Universidad Técnica Estatal de Quevedo and its School of Industrial and Production Sciences for their valuable contribution to the research development of this article.

## **References**

- [1] S. Pinzón, «El perfil alar y su nomenclatura NACA,» rev.ciencia, vol. 1, n° 1, p. 25, 2018.
- [2] E. Ruiz, «Cálculos de los coeficientes aerodinámicos usando MATLAB,» Revista de la Facultad de Ingeniería Industrial, vol. 8, n° 1, p. 9, 2016.
- [3] M. Cesar, «Modelado y simulación aerodinámica de un perfil de microturbina eólica de eje vertical darrieus tipo tres álabes,» vol. 2, n° 1, p. 10, 2017.
- [4] M. Vitorino, «Sistemas Conversores Fluido - Dinámicos de energía renovable para la,» Primera, Argentina, 2016.
- [5] M. Jiménez, «Análisis de un perfil aerodinámico para generar sustentación en la atmósfera de marte,» Primera, Bogotá, 2020.
- [6] A. Gonzáles, «Selección del perfil alar simétrico óptimo para un aerogenerador,» Primera, Córdoba, 2017.
- [7] A. Chipantiza, «Diseño y construcción estructural de un prototipo de avión no tripulado táctico con sistema modular desmontables para el centro de investigación y desarrollo de la fuerza aérea ecuatoriana de la ciudad de Ambato,» Primera, Ambato, 2019.
- [8] A. Dulce, «Aerodinámica no- estacionaria en perfiles de aerogeneradores,» Primera, Madrid, 2016.

- [9] M. Adotti, «Perfiles aerodinámicos: ¿Cómo se diseñan?,» 22 Junio 2020. [En línea]. Available: <https://www.aerodinamicaf1.com/2020/06/perfiles-aerodinamicos-como-se-disenan/>. [Último acceso: 12 08 2021].
- [10] S. Zarea, «Evaluación experimental de ocho perfiles aerodinámicos serie SZ-1500 para bajos número de Reynolds,» vol. 30, n° 2, p. 256, 2016.
- [11] L. Tejada, «Estudio de algunos perfiles aerodinámicos,» Primera, Bogotá, 2020.
- [12] M. Valdez, «Aerodinámica de perfiles con múltiples superficies de control de flujo,» Facultad de ciencias exactas, vol. 5, n° 5, p. 11, 2018.
- [13] D. Ayala, «evaluación por elemento finito de las fuerzas de arrastres y empuje en un perfil Naca,» Primera, Chiapas, 2016.
- [14] D. Salinas, «Medida de fuerzas en túnel aerodinámico sobre perfiles fabricados mediante impresora 3D,» Primera, Cartagena, 2016.
- [15] D. Antonelli, «Simulaciones estacionarias de perfiles aerodinámicos rígidos y flexibles a números de Reynolds ultra-bajos,» Asociación Argentina, vol. 34, n° 8, p. 17, 2016.
- [16] N. Octavio, «Metodología para el modelado y simulación de pruebas de fatiga en álabes de aerogeneradores de baja potencia,» Simulación y laboratorio, vol. 6, n° 20, p. 23, 2019.
- [17] C. Topa y E. Valencia, «Implementation of a Low-Cost Instrumentation for an Open Cycle Wind Tunnel to Evaluate Pressure Coefficient,» World Academy of Science, Engineering and Technology International Journal of Aerospace and Mechanical Engineering, 2018.
- [18] M. Dakel, «Teoría de Mecanismos y máquinas,» Elsevier, vol. 128, p. 707, 2018.
- [19] L. Geovo, «Selección del perfil alar simétrico óptimo para un aerogenerador de eje vertical utilizando la dinámica de flujos computacional,» vol. 12, n° 22, p. 9, 2019.
- [20] J. Murcia, «Aerodinámica de perfiles con borde de salida modificado,» Primera, Bogotá, 2018.
- [21] Q. L. Takao y J. Yusunari, «Effect of solidity on aerodynamic forces around straight-bladed vertical axis wind turbine by wind tunnel experiments (depending on number of blades),» Renewable Energy, pp. 928-939, 2016.